A LETTERS JOURNAL EXPLORING THE FRONTIERS OF PHYSICS

LETTER • OPEN ACCESS

Localization of light in three dimensions: A mobility edge in the imaginary axis in non-Hermitian Hamiltonians

To cite this article: Luca Giuseppe Celardo *et al* 2024 *EPL* **145** 35002

View the article online for updates and enhancements.

You may also like

- Localization transitions and mobility edges in quasiperiodic ladder
R Wang, X M Yang and Z Song
- Many-body localization in the age of classical computing
Piotr Sierant, Maciej Lewenstein, Antonello Scardicchio et al.
- Investigation of reentrant localization transition in one-dimensional quasi-periodic lattice with long-range hopping
Pei-Jie Chang, Qi-Bo Zeng, Jinghui Pi et al.

This content was downloaded from IP address 134.59.100.11 on 17/07/2025 at 12:57

A Letters Journal Exploring the Frontiers of Physics

February 2024

EPL, **145** (2024) 35002
doi: 10.1209/0295-5075/ad222c

www.epljournal.org

Localization of light in three dimensions: A mobility edge in the imaginary axis in non-Hermitian Hamiltonians

Giuseppe Luca Celardo[1,2(a)], Mattia Angeli[3], Francesco Mattiotti[4] and Robin Kaiser[5]

[1] *Department of Physics and Astronomy, Università di Firenze, CSDC and INFN, Florence section, Via G. Sansone, 1, 50019 Sesto Fiorentino, Italy*
[2] *European Laboratory for Non-Linear Spectroscopy, Università di Firenze - Via Nello Carrara 1, 50019 Sesto Fiorentino, Italy*
[3] *John A. Paulson School of Engineering and Applied Sciences, Harvard University - Cambridge, MA 02138, USA*
[4] *CESQ and ISIS (UMR 7006), University of Strasbourg and CNRS - 67000 Strasbourg, France*
[5] *Université Côte d'Azur, CNRS, Institut de Physique de Nice - 06200 Nice, France*

received 26 May 2023; accepted in final form 24 January 2024
published online 26 February 2024

Abstract – Searching for Anderson localization of light in three dimensions has challenged experimental and theoretical research for the last decades. Here the problem is analyzed through large-scale numerical simulations, using a radiative Hamiltonian, *i.e.*, a non-Hermitian long-range hopping Hamiltonian, well suited to model light-matter interaction in cold atomic clouds. Light interaction in atomic clouds is considered in the presence of positional and diagonal disorder. Due to the interplay of disorder and cooperative effects (sub- and super-radiance) a novel type of localization transition is shown to emerge, differing in several aspects from standard localization transitions which occur along the real energy axis. The localization transition discussed here is characterized by a mobility edge along the imaginary energy axis of the eigenvalues which is mostly independent of the real energy value of the eigenmodes. Differently from usual mobility edges it separates extended states from hybrid localized states and it manifests itself in the large moments of the participation ratio of the eigenstates. Our prediction of a mobility edge in the imaginary axis, *i.e.*, depending on the eigenmode lifetime, paves the way to achieve control both in the time and space domains of open quantum systems.

open access Copyright © 2024 The author(s)

Published by the EPLA under the terms of the Creative Commons Attribution 4.0 International License (CC BY). Further distribution of this work must maintain attribution to the author(s) and the published article's title, journal citation, and DOI.

Introduction. – The interplay of opening and disorder in systems described by non-Hermitian Hamiltonians has been at the center of interest in many research fields, showing that non-hermiticity can strongly affect the response of a system to disorder, inducing many counterintuitive effects [1–11]. On the other hand, Anderson localization [12] has been a beacon to understand closed disordered systems and has been at the focus of an ever increasing research community, ranging from condensed matter to acoustics, optics, and ultra-cold matter waves as well as quantum memories based on cold atoms [13–21]. In the standard Anderson localization problem, an excitation can tunnel to nearest-neighbor sites placed in a regular lattice with disordered on-site energies (diagonal disorder). Depending on the value of the disorder strength, a mobility edge can be present at a specific energy: below this energy the eigenstates are localized, while above they are delocalized.

Extending the concepts developed for Anderson localization to open quantum systems still remains a challenge. Light has been an obvious candidate to study Anderson localization of non-interacting waves, which has triggered continuous efforts since the mid-80s [22–31]. So far, Anderson localization of light in three dimensions,

(a) E-mail: giuseppeluca.celardo@unifi.it (corresponding author)

however, has resisted experimental observation. It has now been shown that pioneering experiments on Anderson localization of light [25–27] do not provide a signature for the Anderson transition in three dimensions [28–32] and the mere existence of an Anderson phase transition for light had even been questioned [33,34]. Localization of light indeed presents many features which strongly differ from the standard Anderson localization of closed systems: i) in typical samples, scatterers have random positions in a three-dimensional volume, leading to positional disorder, ii) light induces complex long-range hopping between the sites, which in the case of two-level systems as scattering medium can lead to cooperative effects such as Dicke sub- and superradiance [35–39], iii) the excitation can escape from the system by photon emission, thus placing the problem of localization of light within the framework of open quantum systems. Both the long-range nature of the hopping and the opening can strongly affect the interplay of disorder and transport. Thus, the possibility to have a transition to localization in such systems is highly non-trivial. Specifically, cooperativity can affect the response of the system to disorder in a drastic way: while superradiant states show robustness to disorder [9,10], in the subradiant subspace long-range interaction is effectively shielded [40,41] and signatures of localization can emerge [6,7,40]. In this letter, we shed new light on the problem of light localization in resonant scattering media by combining the positional disorder studied so far, with the initial ingredient of diagonal (on-site) disorder as considered by Anderson [12]. With the aid of large-scale simulations of up to 50000 atoms relying on a well-known radiative non-Hermitian Hamiltonian [42] able to take the vectorial nature of light into account, we show that the playground of the problem of light localization lies in the complex eigenvalues of the radiative Hamiltonian. Specifically, by analyzing the generalized participation ratio (GPR) of the eigenstates, a widely used figure of merit to study localization transitions, we show that a drastic transition in the behaviour of the GPR occurs at a specific imaginary energy value (decay widths) of the eigenstates. Such transition shares many analogies with what happens at real energy mobility edges and thus reveals the presence of a mobility edge along the imaginary axis in such systems.

The model. – We model light scattering in a 3D cold atomic cloud by considering N atoms randomly distributed inside a cube of volume $V = L^3$, with a spatial density $\rho = N/L^3$. When considering the interaction of atoms with the electromagnetic field, the full vectorial character of light should be taken into account. We will focus on atoms driven on a $s \to p$ dipole radiation transition which can be characterized by three degenerate levels in the excited state (labelled as $\alpha = x, y, z$), each with a transition dipole moment (TDM) equal in coupling strength and perpendicular to the others [34]. Thus, we model each atom as a four-level system, with a ground state $|g\rangle$ and three degenerate excited states $|x\rangle$, $|y\rangle$ and $|z\rangle$. Corresponding TDM matrix elements are $\langle\alpha|\widehat{\vec{\mu}}|g\rangle = \mu\hat{e}_\alpha$, with $\alpha = x, y, z$ and the Cartesian unit vectors defined as $\hat{e}_\alpha$. The radiative Hamiltonian $\mathcal{H}_{\rm vec}$ describing dipole-dipole coupling in the single-excitation approximation (see also [42]) is

$$\mathcal{H}_{\rm vec} = \sum_{n=1}^{N} \sum_{\alpha\in\{x,y,z\}} \left(E_{n,\alpha} - i\frac{\Gamma_0}{2}\right) |n,\alpha\rangle\langle n,\alpha| - \frac{\Gamma_0}{2} \sum_{\substack{m,n=1 \\ (m\neq n)}}^{N} \sum_{\alpha,\beta\in\{x,y,z\}} V_{m,n,\alpha,\beta} |m,\alpha\rangle\langle n,\beta|, \quad (1)$$

where $E_{n,\alpha}$ are the atomic transition energies and Γ_0 is the radiative decay rate of a single atom. In eq. (1), $|n,\alpha\rangle$ represents a quantum state where the n-th atom is excited in its α-th state, while all the other atoms are in their ground state. Interaction terms are non-Hermitian, namely,

$$V_{m,n,\alpha,\beta} = \frac{3}{2} e^{ik_0 r_{m,n}} \left[\left(\frac{1}{k_0 r_{m,n}} + \frac{i}{k_0^2 r_{m,n}^2} - \frac{1}{k_0^3 r_{m,n}^3} \right) \hat{e}_\alpha \cdot \hat{e}_\beta - \left(\frac{1}{k_0 r_{m,n}} + \frac{3i}{k_0^2 r_{m,n}^2} - \frac{3}{k_0^3 r_{m,n}^3} \right) \times (\hat{e}_\alpha \cdot \hat{r}_{m,n})(\hat{e}_\beta \cdot \hat{r}_{m,n}) \right]. \quad (2)$$

In eq. (2), $k_0 = 2\pi/\lambda = E_0/(\hbar c)$ is the transition wave number (where λ is the wavelength of the atomic transition and E_0 is the average single atomic transition energy $E_0 = \langle E_{n,\alpha}\rangle$, where the average is taken over disorder realization). $r_{m,n}$ is the distance between the m-th and n-th atom and $\hat{r}_{m,n}$ is the unit vector joining them. Together with the vectorial model we also consider the scalar model [43]. Even though the latter approximation neglects polarisation effects, it is appropriate in the dilute limit, where inter-atomic distances are larger than the optical wavelength λ, making near-field terms decaying as $1/r^3$ negligible (see the Supplementary Material `Supplementarymaterial.pdf` (SM)). The effective Hamiltonian which governs the interaction of the atoms with the electromagnetic field in the scalar approximation is characterized by complex long-range hopping terms $V_{m,n}$ decreasing as $1/r_{m,n}$ with the distance,

$$\mathcal{H} = \sum_{n=1}^{N} \left(E_n - i\frac{\Gamma_0}{2}\right) |n\rangle\langle n| - \frac{\Gamma_0}{2} \sum_{m\neq n}^{N} V_{m,n} |m\rangle\langle n|, \quad (3)$$

where the state $|n\rangle$ stands for the n-atom in the excited state and all the other atoms are in the ground state, while $V_{m,n} = \frac{\exp(ik_0 r_{m,n})}{k_0 r_{m,n}}$ is the interaction between the atoms at distance $r_{m,n}$. The model in eq. (3), known as the scalar model, has been introduced first by Foldy [44] and it has been used in several papers to describe cold atomic

clouds in the dilute limit [45]. Note that the vectorial model Hamiltonian has dimension $3N \times 3N$ contrary to the scalar case which has dimension $N \times N$. Thus, the scalar model allows us to investigate much larger system sizes with better statistics. For both models we can define the resonant mean free path $l = 1/\rho\sigma_0$ (in the independent scattering approximation), where $\sigma_0 = 4\pi/k_0^2$ is the resonant scattering cross-section in a simplified scalar model. Finally, we define the resonant optical thickness, b_0, as the ratio between the system size L and the mean free path l. For the scalar model we have

$$b_0 = \frac{L}{l} = \frac{4\pi\rho^{2/3}N^{1/3}}{k_0^2}, \tag{4}$$

while for the vectorial model the resonant scattering cross-section is $\sigma_0 = 6\pi/k_0^2$ and the optical thickness thus has to be corrected with respect to the scalar case: $b_0^{(\mathrm{vec})} = (3/2)b_0^{(\mathrm{scal})}$.

Note that $\mathcal{H}$ contains both real and imaginary parts, which takes into account that the excitation is not conserved since it can leave the system by outgoing radiation. Its complex eigenvalues $\mathcal{E} = E - i\Gamma/2$ describe the energies and linewidths (decay rates) of the eigenmodes of the system. We stress that even in the dilute limit $\rho\lambda^3 \ll 1$ we can have cooperative behaviour in the large sample limit ($L \gg \lambda$), provided that the cooperativity parameter is $b_0 \gg 1$. In this regime cooperative effects such as single-excitation sub- and superradiance become relevant [37,45,46].

In addition to the positional disorder of the atoms as studied previously [33,34], we now introduce an additional random diagonal disorder term in the Hamiltonian, which shifts the excitation energy of the atoms around its average value E_0. Such diagonal disorder terms have not been given sufficient consideration in the context of localization of light, as engineering such effects is difficult in typical condensed-matter samples. However, in cold atomic clouds, such on-site disorder can be realized by applying a speckle field coupling the excited state to an auxiliary excited state with convenient detuning, inducing thus random light shifts of the atomic resonances without inducing dipole forces in the ground state. Following the approach of the Anderson model on a lattice, we allow the site energies to fluctuate with uniform probability around the natural excitation energy in the range of $[-W/2, +W/2]$, where W is the strength of disorder. We recall that, in addition to this diagonal disorder, we also include positional disorder which has been implemented by choosing the position of the atoms randomly with uniform probability inside a cube of side L. Ensemble averaging thus includes different realizations of the random position of the atoms and of site disorder. Within this model, we study both the eigenvalues as has been done in [33,34] as well as the eigenstates [47].

Localized subradiant states. – A striking illustration of the existence of localized states is given in fig. 1,

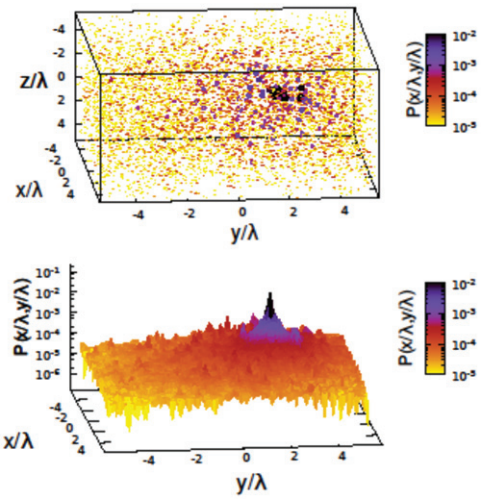

Fig. 1: Localized subradiant eigenstates. A typical localized subradiant state for the scalar model and for $\Gamma = 0.094\Gamma_0, E = 0.1\Gamma_0$ and a participation ratio $PR_2 \approx 7$ for the case $W/(\Gamma_0 b_0) = 0.4$ and $N = 6400, \rho\lambda^3 = 5$ so that $b_0 \approx 17.3$. Upper panel: three-dimensional representation of a localized eigenstate. The radius representing each atom is proportional to its excitation probability $|\Psi_j(r)|^2$, also coded in color (see SM). Lower panel: a localized eigenstate projected on the x-y plane.

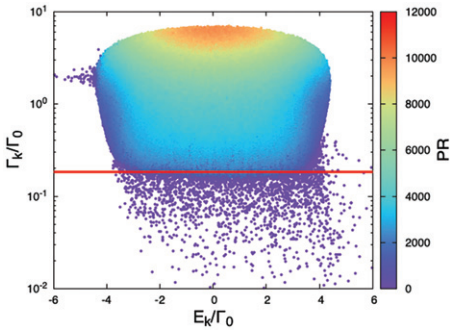

Fig. 2: Participation ratio in the complex plane: the participation ratio $PR = PR_{q=2}$ of the eigenstates for the scalar model is shown in the complex plane (E_k, Γ) of the complex eigenvalues for $N = 28^3$, $\rho\lambda^3 = 5$, $b_0 \approx 26.06$ and $W/(b_0\Gamma_0) = 0.3$. The critical width for the transition to localization (eq. (7)) is indicated by the red horizontal line. Note that E_k is the difference between the real part of the eigenvalues and E_0.

where we represent a typical localized subradiant eigenstate for the scalar model. The upper panel of fig. 1 shows a 3D representation of a typical localized eigenstate, while the lower panel of fig. 1 shows the projection of the squared wave function $|\psi(r)|^2$ on the x-y plane. While for zero diagonal disorder the vast majority of the states, which can be both superradiant or subradiant, are fully delocalized (see SM) for the spatial density considered, adding sufficient diagonal disorder leads to localization of the longer-lived subradiant states. We observe that the localized peak, shown in the lower panel of fig. 1, comes

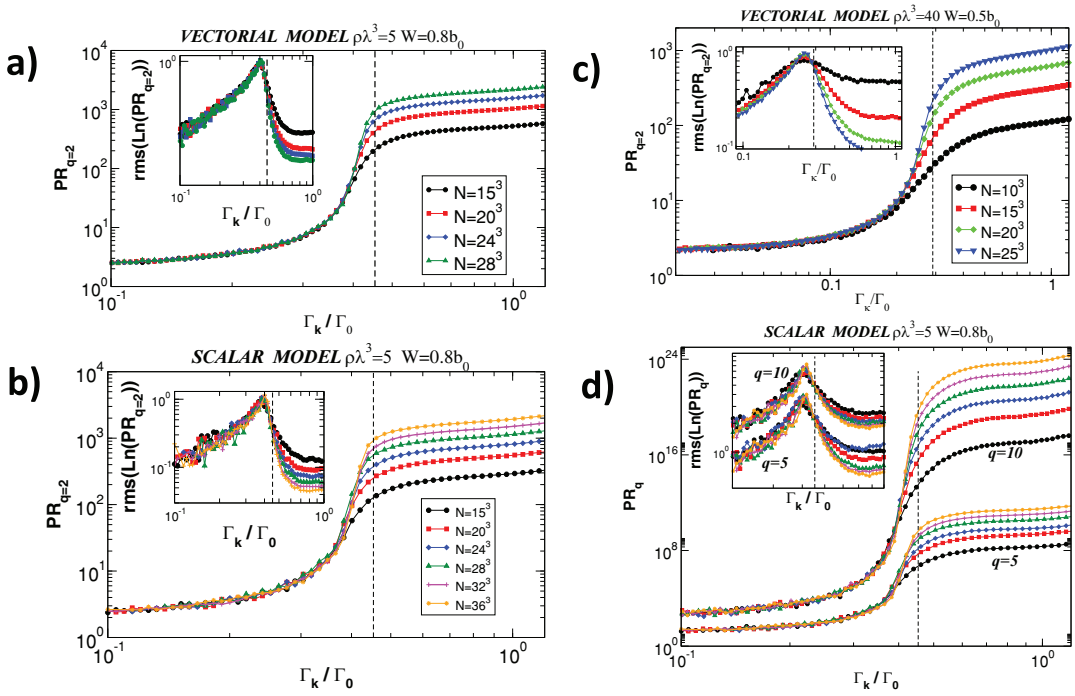

Fig. 3: Mobility edge in the imaginary axis. Typical GPR for $q = 2$ (panel (a), (b), (c)) and $q = 5, 10$ (panel (d)) as a function of the decay width of the eigenstates are shown both for the vectorial ((a), (c)) and scalar model ((b), (d)) for different number N of atoms and constant density, see legend. The vertical black dashed line indicates the critical width (eq. (7)). In the insets the root mean square of $\ln(PR_q)$ is shown as a function of the decay width of the eigenstates. In panels (a), (b), (d), for each N the eigenvalues in the region $-b_0/4 < (E - E_0)/\Gamma_0 < b_0/4$ were considered, while in panel (c) those in the region $-7 - b_0/4 < (E - E_0)/\Gamma_0 < 7 + b_0/4$ were considered.

hand in hand with an extended tail, thus exhibiting a hybrid character, in agreement with refs. [6,7,40]. We note that the presence of such extended tails might strongly affect transport properties [48], for instance suppressing the exponential decay of transmission with the system size. Here we focus on the structure of the eigenmodes, leaving the analysis of the transport properties of subradiant localized states for a future work.

Mobility edge in the imaginary axis. – In open systems, standard approaches to study localization such as the Thouless parameter should be applied with care [49]. We therefore analyze the properties of the generalized participation ratio (GPR) of the eigenfunction ψ of the system [50,51],

$$PR_q = \left| \sum_i |\langle i|\psi\rangle|^2 \right|^q \Big/ \sum_i |\langle i|\psi\rangle|^{2q}. \tag{5}$$

For localized eigenfunctions PR_q is independent of the system size for all q, while in the delocalized regime $PR_q \propto N^{q-1}$. On the other hand, at the localization transition the GPR diverges with N as

$$PR_q \propto N^{D_q(q-1)/d}, \tag{6}$$

where d is the embedding dimension and D_q defines the fractal dimension. Moreover, the distribution $P(PR_q/PR_q^{typ})$, where $PR_q^{typ} = \exp\langle \ln(PR_q)\rangle$, is invariant at criticality in the large system size limit. This implies that the variance of the distribution $P(\ln(PR_q))$ is independent of the size at criticality [52–59], allowing for a precise identification of the critical point.

In order to have a general view of the localization properties of the eigenmodes of our system, we computed the GPR of all the eigenmodes for a specific disorder strength, and we plotted them as a function of their complex eigenvalues (real and imaginary parts). A typical example of this analysis can be seen in fig. 2, which shows a strong dependence of the PR_2 of the eigenmodes on the imaginary part of their eigenvalues, while the dependence on the real part is weak. Specifically we observe that the smaller their imaginary part is, the more the eigenmodes are localized. Note that the results of fig. 2 refer to the scalar model, and a similar figure for the vectorial model can be found in the SM. These results are consistent with previous findings about the interplay of super- and subradiance with disorder [6,7,9,10]: subradiant states are the ones which are most affected by disorder. The most interesting feature of this non-uniform response of the eigenmodes to disorder can be seen if one analyzes the typical value of PR_q (PR_q^{typ}) as a function of the decay widths. Since the optical thickness b_0 sets a relevant energy scale of the system (*i.e.*, the spectral energy broadening prior to adding the diagonal disorder) [34], we considered different

systems at a constant density and for a fixed value of the ratio $W/(b_0\Gamma_0)$. The results are shown in fig. 3, both for the vectorial and the scalar model, for different system sizes at constant density. The results clearly indicate the presence of a transition in the behaviour of the GPR: while the typical PR_q of the eigenmodes is independent of the system size below $\Gamma_{\rm cr}$ if W/b_0 is kept fixed (see vertical dashed line), it increases with the system size above $\Gamma_{\rm cr}$. These are precisely the same features present when analyzing the GPR of the 3D Anderson model (or other models displaying a localization transition) in correspondence of a mobility edge in the real energy. Thus, our results points to the existence of a "mobility edge" in the imaginary axis. We checked that the imaginary mobility edge is independent of E around the band center, as shown in fig. 2 and further discussed in the SM.

We note that in the large density limit the results shown in fig. 3(c) are extremely interesting, since they indicate that in the presence of diagonal disorder, a localization transition can exist even in the large density limit for the vectorial case in the absence of any magnetic field. This is at variance with what has been stated in [33] where no diagonal disorder was considered. Moreover, the mobility edge in the imaginary axis, even in the large density limit, is well captured by eq. (7).

In order to identify the critical decay width corresponding to the imaginary mobility edge, we performed a systematic analysis of the variance of the GPR *vs.* the disorder strength W/Γ_0 for different densities, system sizes and ranges of decay widths. The variance of $\ln(PR_q)$ has been used in the literature to pinpoint the localization transition and it has been shown that, at the localization transition, the variance of $\ln(PR_q)$ is independent of the system size due to a universal distribution of the GPR [54]. Similarly to ref. [59], we use the crossing of $\mathrm{rms}(\ln PR_q)$ close to its maximal value to locate the localization transition, see insets in fig. 3. This allowed us to identify a critical decay width Γ_{cr}.

We studied the critical decay widths as a function of disorder for different densities. The results are shown in fig. 4(a). By fitting the numerical results we obtained an expression for the critical decay width:

$$\frac{\Gamma_{\rm cr}}{\Gamma_0} \approx 0.021 + 0.54\frac{W}{b_0\Gamma_0}. \qquad (7)$$

We note that the above expression cannot be extrapolated at small values of disorder since in that case the landscape of the GPR can only be understood analysing the whole complex plane (see SM).

We have also analyzed the GPR for different q values: $q = 0.1, 0.6, 2, 5, 10$ (see SM). For $q \geq 2$ we always find a clear signature of a localization transition at a critical decay width, while for small values of q a localization transition is not observed. This reflects the hybrid nature of the localized eigenstates: indeed together with a localized peak, an extended tail is present. The GPR for large values of q is more sensitive to large values of $|\psi|^2$, thus it

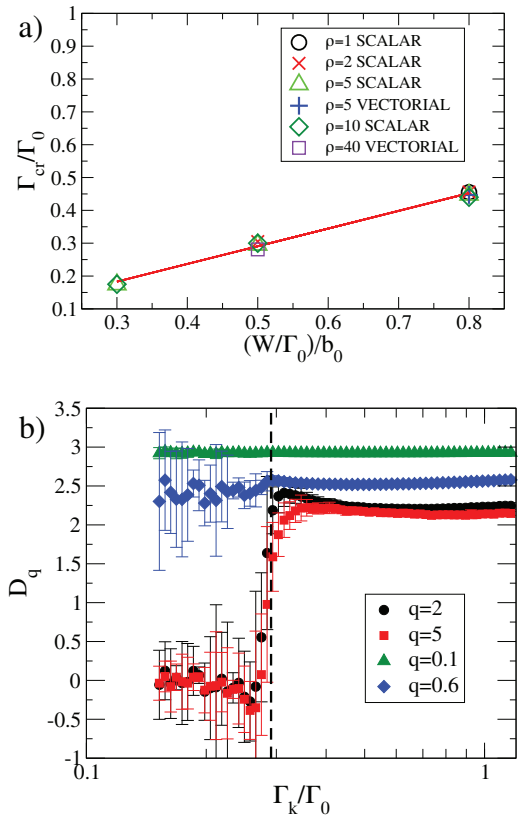

Fig. 4: Panel (a): critical decay width. The critical decay width for the localization transition is shown as a function of the normalized disorder strength for different densities and for both the vectorial and the scalar model (see legend). The precision with which we determined the critical decay width is always below ± 0.015. Panel (b): fractal dimension. The fractal dimension as a function of the normalized decay width is shown for the case $\rho\lambda^3 = 5$, $W/(b_0\Gamma_0) = 0.5$. The fractal dimension has been extracted from the size dependence of the GPR for different values of q. The vertical black dashed line indicates the critical width (eq. (7)).

describes the behaviour of the localized peak, whereas the GPR for small values of q is sensitive to small values of the wave function amplitudes and thus to the wave function tails. Since the tails are always extended (delocalized), no localization transition is seen for small q (see SM). In order to further confirm the above picture, we have computed the fractal dimension D_q as a function of the decay widths. The results are shown in fig. 4(b). As one can see for $q \geq 2$ a transition in the fractal dimension is seen from zero to a value larger than one, while for $q < 1$ no transition is observed, confirming the hybrid nature of the eigenmodes of the system. Note that in the extended phase, even for $q = 2, 5$, D_q is different from $d = 3$ indicating that the wave functions are never fully extended. In other words, the eigenfunctions are always multifractal both below and above criticality: $\Gamma_{\rm cr}$ marks the transition from a frozen phase (where the the GPR is independent of N for sufficiently large q), to a weakly multifractal phase (with a narrow distribution of fractal dimensions D_q) [60].

Conclusions. – We considered a well-known radiative non-Hermitian Hamiltonian model to describe coherent multiple scattering of light in cold atomic clouds at low excitation level. Our results give new insights into the problem of localization in open quantum systems under the interplay of non-hermiticity and disorder. A novel kind of localization transition has been identified, occurring at a critical lifetime (or inverse decay rate Γ) of the eigenmodes of the system, *i.e.*, along the imaginary energy axis. A single-parameter scaling was found for the critical decay rate Γ_{cr}/Γ_0 (eq. (7)) for the localization transition, which is given by $W/(b_0\Gamma_0)$, in contradiction to what could be expected from ρ or b_0 separately. The localization transition identified here in a realistic model of light matter interaction shares many analogies with the Anderson transition in 3D lattices and with localization transitions in long-range interacting systems, such as in the power-banded random matrix model [54,60], but also important differences: the localization transition is signalled by the behaviour of the GPR for large q values (larger than or equal to 2) and not for small q values (less than 2). We attribute this feature to the fact that the eigenmodes are not fully localized but that they have a hybrid character, with a localized peak and an extended tail. A precise characterization of the shape of these eigenmodes will be the topic of a future work. Despite these differences, our results indicate the existence of a novel kind of localization transition occurring along the imaginary energy axis which is independent of the real energy (around the band center) for sufficiently large values of diagonal disorder and optical thickness. The existence of a mobility edge in the imaginary axis found in this letter certainly constitutes a novel feature in the field of localization in open quantum systems. Further research will be necessary to assess the impact of our results. For instance the general conditions for this mobility edge in the imaginary axis to arise in open quantum systems should be investigated both in the single excitation and many excitation regime, as well as for different topology and dimensions. In addition the corresponding critical exponents remain to be determined. It would also be interesting to explore the sensitivity of the mobility edge along the imaginary axis to the boundary conditions and its relation to the non-Hermitian skin effect [61]. Our findings are relevant not only from a fundamental point of view but also for applications, *e.g.*, to achieve efficient energy storage, quantum memory, quantum simulation and sensing devices.

* * *

We acknowledge stimulating discussions with R. Bachelard, A. Biella, F. Borgonovi, G. G. Giusteri and W. Guerin. Computing time was provided by the High Performance Computing Center of the University of Strasbourg. This research was also supported, in part, by the Center for Research Computing of the University of Notre Dame through access to key computational resources. Part of this work was performed in the framework of ERC Advanced Grant No. 832219 (ANDLICA). GLC acknowledges financial support from PNRR MUR project PE0000023-NQSTI.

Data availability statement: All data that support the findings of this study are included within the article (and any supplementary files).

REFERENCES

[1] Eichelkraut T., Heilmann R., Weimann S., Stützer S., Dreisow F., Christodoulides D. N., Nolte S. and Szameit A., *Nat. Commun.*, **4** (2013) 2533.
[2] Luo X., Ohtsuki T. and Shindou R., *Phys. Rev. Lett.*, **126** (2021) 090402.
[3] Kawabata K. and Ryu S., *Phys. Rev. Lett.*, **126** (2021) 166801.
[4] Huang Y. and Shklovskii B. I., *Phys. Rev. B*, **101** (2020) 014204.
[5] Weidemann S., Kremer M., Longhi S. and Szameit A., *Nat. Photon.*, **15** (2021) 576.
[6] Celardo G., Biella A., Kaplan L. and Borgonovi F., *Fortschr. Phys.*, **61** (2013) 250.
[7] Biella A., Borgonovi F., Kaiser R. and Celardo G. L., *EPL*, **103** (2013) 57009.
[8] Cottier F., Cipris A., Bachelard R. and Kaiser R., *Phys. Rev. Lett.*, **123** (2019) 083401.
[9] Celardo G. L., Giusteri G. G. and Borgonovi F., *Phys. Rev. B*, **90** (2014) 075113.
[10] Giusteri G. G., Mattiotti F. and Celardo G. L., *Phys. Rev. B*, **91** (2015) 094301.
[11] Celardo G. L. and Kaplan L., *Phys. Rev. B*, **79** (2009) 155108.
[12] Anderson P. W., *Phys. Rev.*, **109** (1958) 1492.
[13] Lee P. A. and Ramakrishnan T. V., *Rev. Mod. Phys.*, **57** (1985) 287.
[14] Akkermans E. and Montambaux G., *Mesoscopic Physics of Electrons and Photons* (Cambridge University Press) 2007.
[15] Lagendijk A., van Tiggelen B. and Wiersma D., *Phys. Today*, **62**, issue No. 8 (2009) 24.
[16] Aspect A. and Inguscio M., *Phys. Today*, **62**, issue No. 8 (2009) 30.
[17] Hu H., Strybulevych A., Page J., Skipetrov S. E. and van Tiggelen B. A., *Nat. Phys.*, **4** (2008) 945.
[18] Chabé J., Lemarié G., Grémaud B., Delande D., Szriftgiser P. and Garreau J. C., *Phys. Rev. Lett.*, **101** (2008) 255702.
[19] Kondov S. S., McGehee W. R., Zirbel J. J. and DeMarco B., *Science*, **334** (2011) 66.
[20] Jendrzejewski F., Bernard A., Mueller K., Cheinet P., Josse V., Piraud M., Pezzé L., Sanchez-Palencia L., Aspect A. and Bouyer P., *Nat. Phys.*, **8** (2012) 398.
[21] Semeghini G., Landini M., Castilho P., Roy S., Spagnolli G., Trenkwalder A., Fattori M., Inguscio M. and Modugno G., *Nat. Phys.*, **11** (2015) 554.
[22] John S., *Phys. Rev. Lett.*, **53** (1984) 2169.
[23] John S., *Phys. Rev. Lett.*, **58** (1987) 2486.
[24] Anderson P. W., *Philos. Mag. B*, **52** (1985) 505.

[25] Wiersma D. S., Bartolini P., Lagendijk A. and Righini R., *Nature*, **390** (1997) 671.
[26] Aegerter C. M., Störzer M. and Maret G., *EPL*, **75** (2006) 562.
[27] Sperling T., Buehrer W., Aegerter C. M. and Maret G., *Nat. Photon.*, **7** (2013) 48.
[28] Scheffold F., Lenke R., Tweer R. and Maret G., *Nature*, **398** (1999) 206.
[29] van der Beek T., Barthelemy P., Johnson P. M., Wiersma D. S. and Lagendijk A., *Phys. Rev. B*, **85** (2012) 115401.
[30] Scheffold F. and Wiersma D., *Nat. Photon.*, **7** (2013) 934.
[31] Sperling T., Schertel L., Ackermann M., Aubry G. J., Aegerter C. M. and Maret G., *New J. Phys.*, **18** (2016) 013039.
[32] Skipetrov S. E. and Page J. H., *New J. Phys.*, **18** (2016) 021001.
[33] Skipetrov S. E. and Sokolov I. M., *Phys. Rev. Lett.*, **112** (2014) 023905.
[34] Bellando L., Gero A., Akkermans E. and Kaiser R., *Phys. Rev. A*, **90** (2014) 063822.
[35] Akkermans E., Gero A. and Kaiser R., *Phys. Rev. Lett.*, **101** (2008) 103602.
[36] Kaiser R., *J. Mod. Opt.*, **56** (2009) 2082.
[37] Bienaimé T., Piovella N. and Kaiser R., *Phys. Rev. Lett.*, **108** (2012) 123602.
[38] Akkermans E. and Gero A., *EPL*, **101** (2013) 54003.
[39] Guerin W., Rouabah M. and Kaiser R., *J. Mod. Opt.*, **64** (2017) 895.
[40] Celardo G. L., Kaiser R. and Borgonovi F., *Phys. Rev. B*, **94** (2016) 144206.
[41] Santos L. F., Borgonovi F. and Celardo G. L., *Phys. Rev. Lett.*, **116** (2016) 250402.
[42] Mattiotti F., Kuno M., Borgonovi F., Jankó B. and Celardo G. L., *Nano Lett.*, **20** (2020) 7382.
[43] Cipris A., Bachelard R., Kaiser R. and Guerin W., *Phys. Rev. A*, **103** (2021) 033714.
[44] Foldy L. L., *Phys. Rev.*, **67** (1945) 107.
[45] Guerin W., Araújo M. O. and Kaiser R., *Phys. Rev. Lett.*, **116** (2016) 083601.
[46] Araújo M. O., Krešić I., Kaiser R. and Guerin W., *Phys. Rev. Lett.*, **117** (2016) 073002.
[47] Máximo C. E., Piovella N., Courteille P. W., Kaiser R. and Bachelard R., *Phys. Rev. A*, **92** (2015) 062702.
[48] Chávez N. C., Mattiotti F., Méndez-Bermúdez J. A., Borgonovi F. and Celardo G. L., *Phys. Rev. Lett.*, **126** (2021) 153201.
[49] Wang J. and Genack A. Z., *Nature*, **471** (2011) 345.
[50] Rodríguez A., Malyshev V. A. and Domínguez-Adame F., *J. Phys. A*, **33** (2000) L161.
[51] Rodríguez A., Malyshev V. A., Sierra G., Martín-Delgado M. A., Rodríguez-Laguna J. and Domínguez-Adame F., *Phys. Rev. Lett.*, **90** (2003) 027404.
[52] Cuevas E., *Phys. Rev. B*, **66** (2002) 233103.
[53] Cuevas E., Ortuño M., Gasparian V. and Pérez-Garrido A., *Phys. Rev. Lett.*, **88** (2001) 016401.
[54] Mildenberger A., Evers F. and Mirlin A. D., *Phys. Rev. B*, **66** (2002) 033109.
[55] Evers F. and Mirlin A. D., *Phys. Rev. Lett.*, **84** (2000) 3690.
[56] Varga I., *Phys. Rev. B*, **66** (2002) 094201.
[57] Méndez-Bermúdez J. A., Alcázar-López A. and Varga I., *EPL*, **98** (2012) 37006.
[58] Méndez-Bermúdez J. A., Alcazar-López A. and Varga I., *J. Stat. Mech.: Theory Exp.*, **2014** (2014) P11012.
[59] Vega-Oliveros D. A., Méndez-Bermúdez J. A. and Rodrigues F. A., *Phys. Rev. E*, **99** (2019) 042303.
[60] Evers F. and Mirlin A. D., *Rev. Mod. Phys.*, **80** (2008) 1355.
[61] Lin R., Tai T., Li L. and Lee C. H., *Front. Phys.*, **18** (2023) 53605.